

## **Section 2**

# **ADVANCED TECHNOLOGY DEVELOPMENTS**

### **2.A Optical Probes for the Characterization of Surface Breakdown**

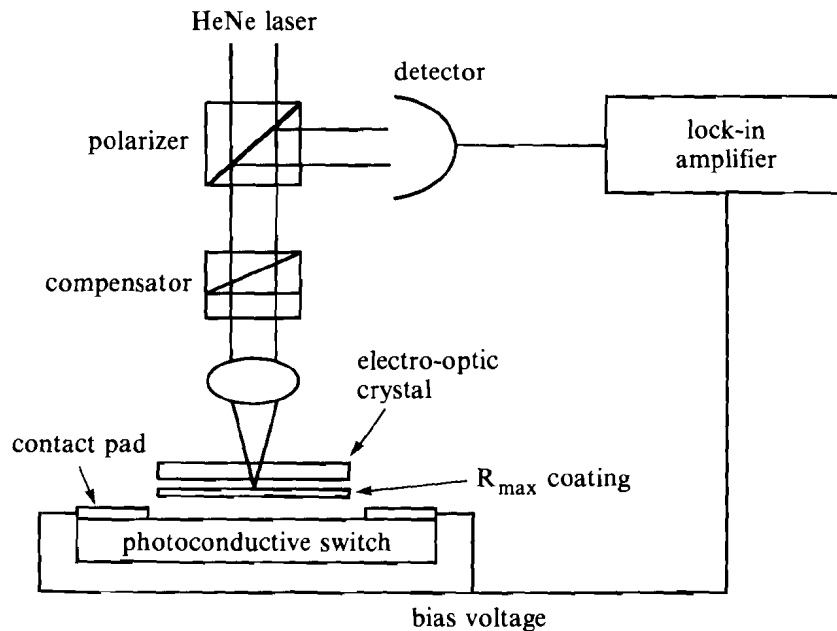
The driving force behind this investigation is the need to understand surface breakdown on semiconductors. Many applications require that electrodes on semiconductor materials be placed in geometries where significant electric fields are developed across their surfaces. This generalization is true over a wide range of applications. High-speed semiconductor circuits, such as those in very large scale integration (VLSI) applications, place relatively small voltages across the electrodes, but the electrode separation is made as small as possible to reduce the signal propagation time through the device. This results in large electric fields. Pulsed-power semiconductor switches have relatively large electrode separations, but they are required to hold off very large voltages. Surface breakdown is the major limiting factor in the operation of these elements. Whether the circuits are for high-speed logic or pulse power, the need to keep the surface electric fields below the level where surface breakdown will occur places a minimum-size restriction on the devices that can be constructed. Despite its relevance, the mechanism of surface breakdown on most materials is poorly understood. Semiconductors in particular are difficult to understand because of the presence of free carriers on the surface that modify the distribution of the electric field. This report presents the development of an imaging technique to monitor the temporal evolution of surface electric fields. These experiments seek to use this information to reconstruct the dynamics of the charge carriers on the semiconductor surface.

The electro-optic, or Pockels, effect is a novel probe of surface electric fields.<sup>1</sup> It can modulate an optical probe to produce an optical replica of the electric field under investigation. The unique features of electro-optic sampling are its speed and noninvasive nature. The response time of the electro-optic material is of the order of femtoseconds, which allows for extremely high bandwidth signal acquisition. In addition, electro-optic sampling techniques have measured electrical rise times as short as 300 fs without loading the circuit.<sup>2</sup> Because the probe is optical, no electrical contacts, which can perturb the device under test, are needed. The optical coupling also means that the detection electronics are isolated from any dangerous high-voltage transients at the test circuit.

**Electro-Optic Probing**

An electro-optic crystal placed in the fringing electric field above the semiconductor surface experiences a change in its birefringence as a function of the electric field. The change in the birefringence is monitored by probing the crystal with polarized light, as shown in Fig. 34.18. The light passes through a polarizer; a waveplate, to provide an adjustable bias to the transmission; the electro-optic crystal; and then reflects off a dielectric mirror to retrace its path. Because of the waveplate, the polarizer is effectively crossed with respect to itself. The Pockels effect can be viewed as the mixing of a dc electric field and an optical field in a crystal to produce a new optical field with its polarization rotated with respect to the original optical field. When the

Fig. 34.18  
Surface field tester for photoconductive switches.



Z265

crystal is placed between crossed polarizers, the transmission is given by

$$T = \sin^2\{(K E d\chi) + \phi\}/2, \quad (1)$$

where  $E$  is the magnitude of the dc electric field,  $d\chi$  is the optical path length through the crystal,  $\phi$  is a constant optical rotation due to the waveplate and static birefringence of the crystal, and  $K$  is a constant that depends on material parameters, the crystal orientation, and the frequency of the optical field.<sup>3</sup> By choosing the type of crystal and its orientation, the Pockels effect can be made sensitive to only one spatial component of the applied electric field.

The dielectric mirror is bonded directly to the electro-optic crystal and the entire assembly is placed directly on top of the surface to be monitored, which has two rectangular electrodes separated by a fixed distance. The crystal used in these experiments was LiTaO<sub>3</sub>. Its optic axis was perpendicular to both the direction of light propagation and the edges of the electrodes. Thus, the optic axis was oriented along the electric field lines, and the Pockels effect was sensitive to only the component of the electric field along that axis.

### Detection Systems

The principal assumption of this work is that the measured electric field will not be uniform over the surface being measured. Two configurations have been used to detect the spatial and temporal variations of the electric field. The initial measurements investigated the low-voltage, quasi-static configuration of the surface electric field. A piece of LiTaO<sub>3</sub> was placed across evaporated metal contacts on both silicon and gallium arsenide. A time-varying potential was induced across the contacts, causing a modulation of the birefringence of the LiTaO<sub>3</sub> in both space and time via the Pockels effect. A tightly focused cw HeNe laser, with a spot size of approximately 40  $\mu\text{m}$ , probed the change in birefringence, as illustrated in Fig. 34.18. The spatial profile was obtained by translating the electro-optic crystal and semiconductor so that different points were illuminated by the laser beam. The low voltage applied to these devices produced very weak modulation of the optical signal, requiring that the signal be extracted with phase-sensitive detection. This experiment demonstrated that we could spatially resolve the surface electric field on the surface of the semiconductor.

The data acquired as described above had two serious drawbacks. It lacked temporal resolution, and required that the beam be scanned spatially to acquire the total spatial variation of the field. Such conditions are incompatible with the need to record spatially nonlocal, transient events typical of a surface breakdown. The second phase of our investigation addressed these issues.

Short-pulse laser probes improve the time resolution. A single light pulse from a frequency-doubled, mode-locked, amplified Nd:YAG laser samples the electric field only while it traverses the sampling crystal (approximately 100 ps). This technique works with a single

optical pulse only at field strengths that are comparable with the field necessary to cause the direction of the polarization vector in the sampling crystal to change by one-half wave (approximately 1–10 kV/mm). Otherwise, the optical modulation would be too weak to be extracted without the aid of extensive signal processing. The study of surface breakdown events, where the sample may be damaged on a single shot, requires unambiguous detection in a single shot. With short-pulse lasers, it is possible to take 100-ps snapshots of any given event. A series of snapshots of the surface electric field can be taken to record the temporal variation in the field.

The spatial variation in the surface field can be monitored by illuminating the entire area of interest. Instead of using a single detector and scanning a tightly focused spot, a detector array captures an image of the entire field of interest. Each detector element measures only a small portion of the electric field. This experiment has been carried out using an 512-element, linear intensified diode array. A 2-mm gap with identically prepared gold-coated, laser-annealed contacts on intrinsic silicon (7000  $\Omega$  cm) was pulse biased with a short electrical pulse synchronized with the laser pulse. A 50- $\Omega$  load was placed on the low side of the silicon and the leakage through the material was monitored. The lack of photoconductive switching at the load guaranteed that none of the light coupled through the dielectric mirror into the silicon; it is important that light does not perturb the field. During the actual acquisition of data, the load was attached directly to the ground. The laser illuminated a circular region on the silicon surface, and the detector acquired a one-dimensional slice of the electric field on a line joining the two electrodes midway between the ends of the electrodes. This is the first demonstration of imaging technology applied to electro-optic field measurements.

### Surface Field Distribution

The electric field distribution produced by the electrode distribution used in these experiments is not uniform. It is a common field configuration encountered when fabricating devices on wafers (e.g., coplanar transmission lines between transistors in VLSI circuits or photoconductive switches fabricated on wafer substrates). The field lines in a plane perpendicular to the surface are shown in Fig. 34.19(b). They may be derived from the simple case illustrated in Fig. 34.19(a) by the operation of the conformal transformation<sup>4</sup>

$$z = 2 \ln \left\{ [1 + \sin(w)]^{1/2} + [b_z + \sin(w)]^{1/2} / (b_z - 1)^{1/2} \right\}, \quad (2)$$

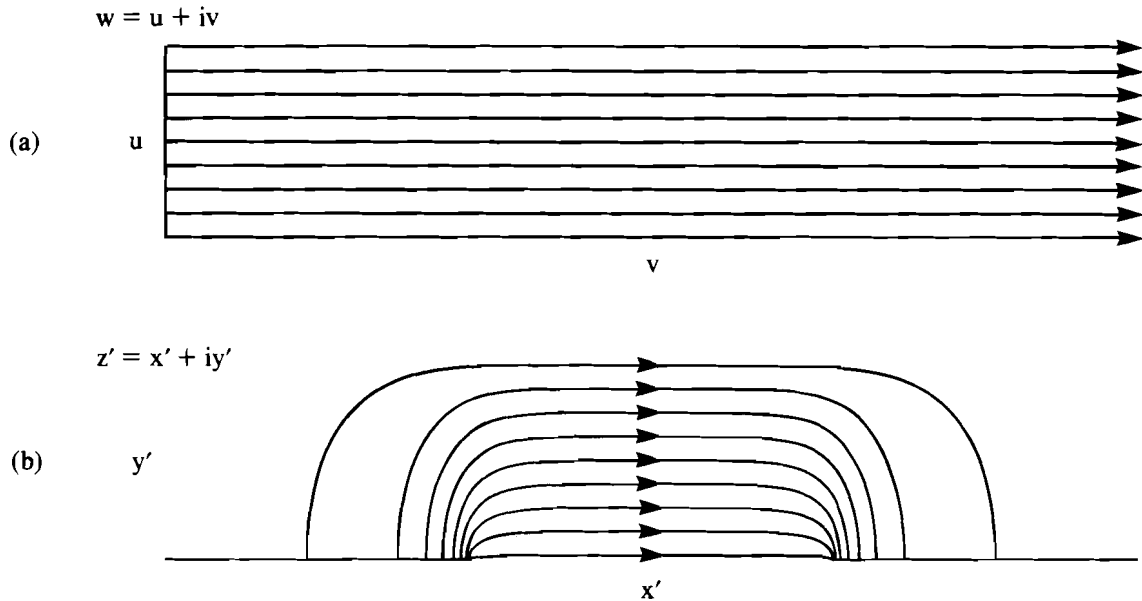
followed by the second transformation

$$z' = w_d - 2 \ln \left\{ \frac{[1 + \sin(iz + \frac{\pi}{2} - iw_g)]^{1/2} + [b_z + \sin(iz + \frac{\pi}{2} - iw_g)]^{1/2}}{(b_z - 1)^{1/2}} \right\}, \quad (3)$$

where

$$b_z = 2 \coth^2 (\pi \ell_c / 2 \ell_s) - 1 \cong 1 \quad (4)$$

$w_g$  is the normalized gap width,  $\ell_c$  is the electrode length,  $\ell_s$  is the substrate thickness,  $w = u + iv$ , and  $z = x + iy$ .



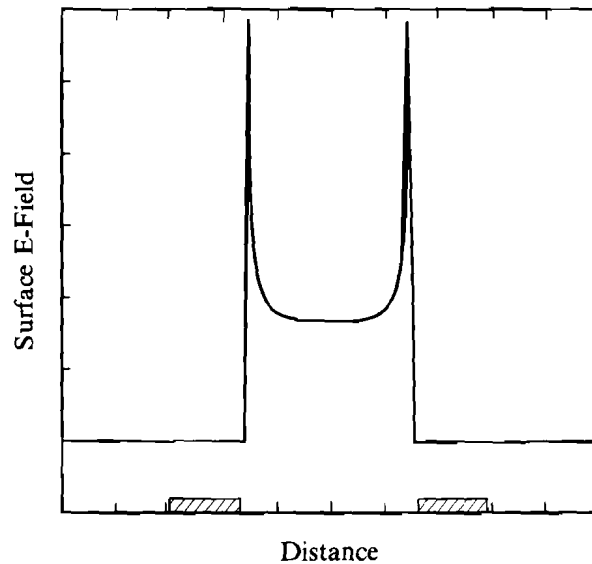
Z434

Fig. 34.19  
Conformal mapping of parallel to coplanar electrodes.

These transformations fold the electrode end faces out into the coplanar geometry. The second transformation is only valid if the transformed plane is at infinite distance from the first plane because the electric field lines must be normal to the second plane. However, if the electrodes are sufficiently far apart, the deviation from normal incidence is negligible. These transformations define the expected value of the electric field throughout the volume of the semiconductor, provided that the measurement is not taken near the corners of the electrodes. The fringing field outside of the semiconductor can be inferred from electromagnetic theory (i.e., the tangential component of the electric field is continuous across a dielectric interface).

From the known electric field configurations in Fig. 34.19(a), the electric field in Fig. 34.19(b) can be calculated. For the type of electro-optic crystal that was used in this experiment, the electric field along the  $x'$  axis in Fig. 34.19(b) was measured. Figure 34.20 shows the field in the plane of the interface; the features are exactly as expected. Above the contacts the electric field is normal to the surface. Therefore, the field along the  $x'$  axis is zero. At the edge of the contacts the field lines bunch up due to the attraction of charges on the opposing electrodes. This is not what is actually measured, however; what is actually measured is the phase shift

$$\theta = \int_{IA} dA \int_0^L KE_{x'}(x, y) dx . \tag{5}$$



Z470

Fig. 34.20  
Surface electric field.

This integral is over the illuminated area ( $IA$ ) and the thickness of the electro-optic crystal ( $L$ ) and is clearly dependent on that thickness. Figure 34.21 shows the integrated detected signal as a function of the electro-optic crystal thickness. The uppermost curve indicates what happens if the crystal is so thick that the integral extends over all the field lines. The surface features are completely obscured because the total integrated flux is conserved between the electrodes. Alternatively, if the crystal is too thin, then the modulation imparted to the light signal becomes very small. The amount of rotation is proportional to the optical path length in the crystal. An intermediate thickness ( $\sim 1/4$  to  $1/5$  of the distance between the electrodes) must be chosen that balances the magnitude of the extracted signal with the smearing due to the path-length integration. Additional smearing of the detected signal is also incorporated into the calculation of the curves in Fig. 34.21. The signal must be averaged over either the laser spot size or the size of the detector element on which it is imaged. In Eq. (5), this is represented by the integral over the illuminated area.

### Results

The usefulness of this technique has been demonstrated at low voltage, where the preparation of the contacts on the semiconductor has been shown to influence the dc electric field distribution. This is the work that was done with the cw probe and the phase-sensitive detection. The primary purpose of the cw experiments was to demonstrate that we could detect spatial variations in the field. The electric field was essentially dc (actually a low-frequency, 1-kHz, square wave). In addition to demonstrating the ability to monitor surface fields, these measurements proved a reliable method of characterizing the contacts. Figure 34.22 shows a cross-sectional view

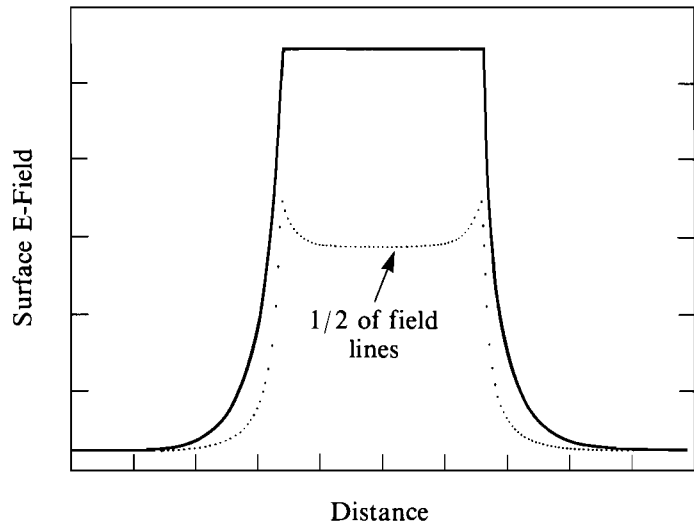


Fig. 34.21  
Integrated surface electric field profile—1/2  
of field lines.

Z428

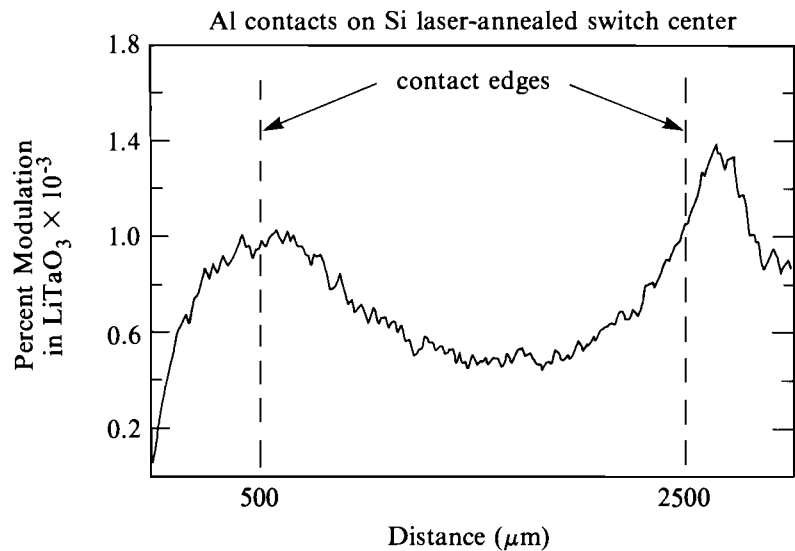


Fig. 34.22  
Surface field profile.

Z283

of the field along the center line between the contact pad on silicon. The figure shows the general features that are expected: the bunching at the contacts and the tailing off at the electrodes. The sampling crystal was thick with respect to the electrode separation. Therefore, the peaks exhibit a significant amount of smearing. What is most interesting is the asymmetry of the electric field. Because the contacts were identically prepared, no asymmetry was expected from the material properties of the sample. When the polarity of the applied

bias was reversed, the asymmetric field distribution also reversed. This indicated that the contacts were not ohmic with respect to the different carrier species (electrons and holes).

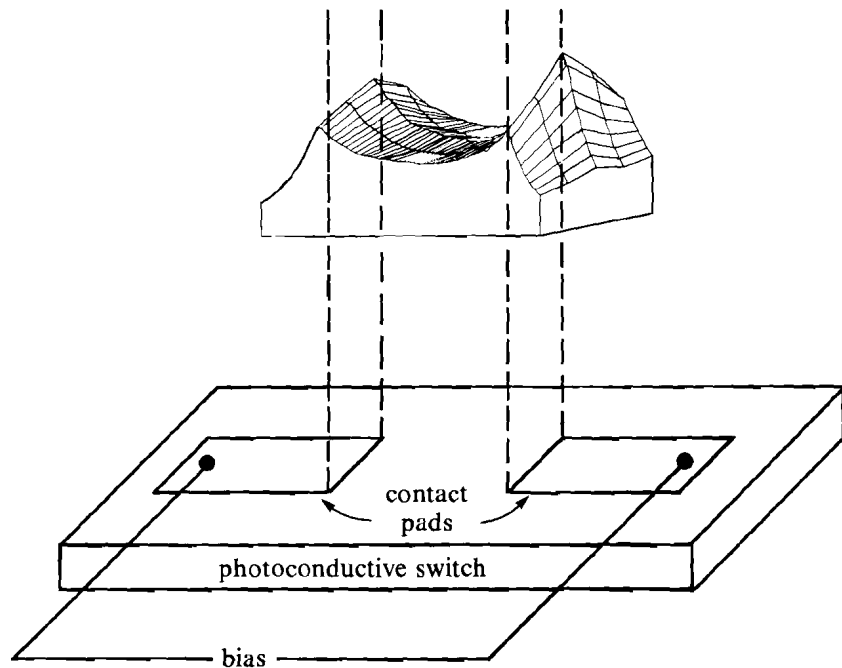
The cw data also showed that a full two-dimensional map of the electric field could be acquired. Figure 34.23 is an axonometric plot of the electro-optic image of the electric field on a silicon switch. The electric field tails off as the probe moves away from the center line of the electrodes.

The time-resolved data was taken to determine the time scale on which the asymmetry illustrated in the cw data evolved. The data was taken by grounding one of the electrodes on a sample prepared on high-resistivity silicon ( $\rho = 7 \text{ k}\Omega \text{ cm} = 70 \text{ }\Omega\text{m}$ ). The dielectric relaxation time of this material is given by the product

$$\rho\epsilon = (70 \text{ }\Omega\text{m} \times 11.9 \times 8.85 \times 10^{-12} \text{ F/m}),$$

where  $\epsilon$  is the dielectric constant of the silicon. Thus, on time scales less than 7 ns, silicon will have a transient response to an applied electric field. A photoconductive switch was used to pulse bias the test structure on a time scale less than 200 ps. One electrode was grounded and the other was attached to a terminated 50- $\Omega$  line driven by a photoconductive switch. The switch was triggered with a 1.06- $\mu\text{m}$  light pulse from a Nd:YAG regenerative amplifier. A 0.532- $\mu\text{m}$  pulse, derived by frequency doubling a portion of the 1.06- $\mu\text{m}$  light, probed the LiTaO<sub>3</sub> crystal. An optical delay line in the path of the 1.06- $\mu\text{m}$  light provided a variable time delay in between the voltage and probe.

Fig. 34.23  
Surface field and contact arrangement.



Z267

The optical image of the electric field was measured with a gated diode array at various time delays between the pump and probe. Figure 34.24 shows three traces of the surface electric field of a device with a 2-mm gap pulsed with 1 kV at various time delays. The units of vertical axis are in percent modulation of the light signal. This is the signal obtained with the voltage on, minus the signal with the voltage off, divided by the signal with the voltage off. Thus, the detected modulation was relatively immune to variations in the illumination profile. At very early times [curve (a)], very little voltage has built up but the device appears to be symmetric in response to the electric field. Curve (b), 166 ps later, shows that a significant voltage has built up across the device and the field is still symmetric. At 332 ps after (a), curve (c) shows that the voltage is still rising but the field displays a definite asymmetry.

The simple explanation of these data is that at early times the electrical inertia of the silicon prevents it from reacting to the field. The device then behaves as if it were a perfect dielectric. The field rises symmetrically on both electrodes and is determined only by the

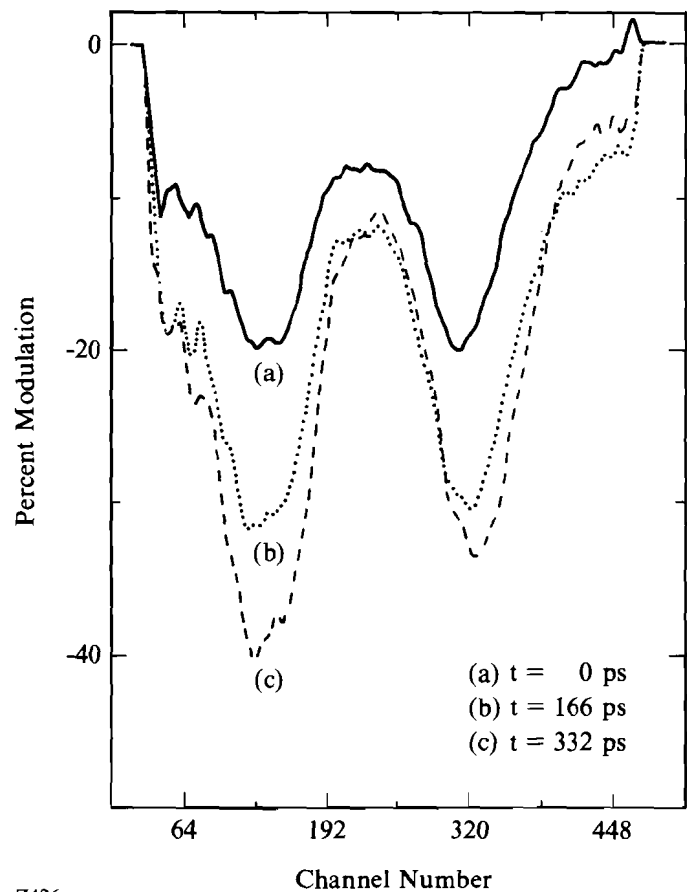


Fig. 34.24  
Surface electric field on silicon versus time.

electrode configuration. Later, as the charge carriers in the silicon begin to rearrange in response to the field, the field itself is modified by the charges in the silicon. Thus, the asymmetry seen in the cw data begins to manifest itself on the time scale of a few hundred picoseconds. This shows that it is possible to probe the transient response of a semiconductor that has been biased on a time scale that is short compared to the dielectric response time of the material.

### Conclusion

At applied fields less than those necessary to cause breakdown, information about the semiconductor device could be readily obtained from the electro-optic imaging data. In the dc biasing case, the contacts were asymmetric with respect to the applied voltage. One contact always had a higher field enhancement at the edge than the other. The enhancement shifted as the polarity of the applied voltage reversed. Such field enhancements are probably due to differences in the injection of holes and electrons at the contacts, and may play an important part in initiating breakdown. The pulse bias case illustrated that this data could be taken on a very short time scale and that transient structure of the electric field can be observed. Although the data shown were averaged over several shots, the 40% modulation can easily be seen in a single shot. By probing at different times and places, we can produce a two-dimensional map of the time evolution of the electric field on a semiconductor surface. Future work will investigate surface breakdown. The electric field will be pulse biased at or near the surface flashover point. The interactions between the electric field and the free carriers can be monitored during a breakdown event. The temporal map of the semiconductor surface field will be taken as described above, with a delay between the pump and probe pulses. An additional feature must be added to the experiment, however. Immediately after the device has been probed with the green pulse, an infrared light pulse will illuminate the device and drive it into the photoconducting state. This will collapse the field and prevent the surface from being destroyed by a surface arc before the full temporal map can be accumulated.

### ACKNOWLEDGMENT

This work was supported by the Laser Fusion Feasibility Project at the Laboratory for Laser Energetics, which has the following sponsors: Empire State Electric Energy Research Corporation, New York State Energy Research and Development Authority, Ontario Hydro, and the University of Rochester. Additional support was provided by SDIO/IST and managed by ONR under contract No. N00014-86-K-0538. Such support does not imply endorsement of the content by any of the above parties.

### REFERENCES

1. K. E. Meyer and G. Mourou, in *Picosecond Electronics and Optoelectronics*, edited by G. A. Mourou, D. M. Bloom, and C. H. Lee (Springer-Verlag, Berlin, 1985), pp. 46-49.
2. J. A. Valdmanis, G. A. Mourou, and G. W. Gabel, *Appl. Phys. Lett.* **41**, 211 (1982).
3. A. Yariv, *Quantum Electronics*, 2nd ed. (John Wiley & Sons, New York, 1975), p. 340.
4. P. M. Hall, *Thin Solid Films* **1**, 277 (1967).